Zoological Journal of the Linnean Society, 2008, **152**, 775–792. With 12 figures

Cranial morphology of *Bachia bicolor* (Squamata: Gymnophthalmidae) and its postnatal development

OSCAR A. TARAZONA[1]*, MARISSA FABREZI[2] and MARTHA PATRICIA RAMÍREZ-PINILLA[3]

[1]*Laboratorio de Biología Reproductiva de Vertebrados, Escuela de Biología, Universidad Industrial de Santander, Bucaramanga, Colombia*
[2]*CONICET, IbiGeo-Museo de Ciencias Naturales, Universidad Nacional de Salta, Mendoza 2, 4400-Salta, Argentina*
[3]*Colección Herpetológica y Laboratorio de Biología Reproductiva de Vertebrados, Grupo de Estudios en Biodiversidad, Escuela de Biología, Universidad Industrial de Santander, Bucaramanga, Colombia*

Received 5 July 2006; accepted for publication 21 June 2007

This study describes the adult cranial osteology of the gymnophthalmid lizard *Bachia bicolor*, and its variation during postnatal development. Descriptions are based on a size series of osteological preparations, including dry skeletons and cleared and double-stained specimens. The adult skull morphology of *B. bicolor* is similar to that of other gymnophthalmids; however, it shows some particular characters that are convergent with those of several serpentiform lizards. The skull design of *B. bicolor* has two remarkable structural modifications: (1) the presence of the basisphenoid rostral process by the ossification of the cartilage trabecula communis during postnatal development, and (2) the broad orbitosphenoid bone. The latter is a compound bone (chondral and membranous) that forms part of the anterior braincase floor. Some of the cranial modifications observed in *B. bicolor* arise during postnatal development, suggesting an important role for possible heterochronic changes. *Zoological Journal of the Linnean Society*, 2008, **152**, 775–792.

ADDITIONAL KEYWORDS: cranial osteology – ontogeny – orbitosphenoid – trabecula communis.

INTRODUCTION

In squamate lizards, several studies have found that morphological patterns such as limb reduction/loss, body elongation, and cranial modifications (loss of skull elements and reduction of head diameter) can be explained by miniaturization and/or fossoriality (Rieppel, 1984, 1996; Lee, 1998). Those patterns are more frequently observed in Scleroglossa, having multiple independent origins in unrelated groups like Amphisbaenia, Dibamidae, Serpentes, Pygopodidae, Anguidae, Scincidae and Gymnophthalmidae (Estes, de Queiroz & Gauthier, 1988; Lee, 1998; Wiens & Slingluff, 2001).

*Corresponding author. E-mail: oscalej@gmail.com

Gymnophthalmid lizards exhibit morphological patterns that at first glance can be regarded as intermediate morphotypes between the saurian and serpentiform body plans, which seemingly would involve processes such as miniaturization and/or fossoriality (Dixon, 1973; Presch, 1975, 1980; Pellegrino *et al*., 2001). Among the members of this group there are forms with small body size, elongated trunks, reduced limbs, and with loss of external ear openings; they are frequently burrowers or fossorial animals. A recent molecular phylogenetic analysis of Gymnophthalmidae supports the hypothesis of multiple independent origins of those characters (Pellegrino *et al*., 2001), confirming the morphological convergence observed in Squamata (Lee, 1998).

Bachia is a genus of gymnophthalmid lizards that shows several degrees of limb reduction, with a wide

range of limb morphologies (Dixon, 1973; Presch, 1975; Kizirian & McDiarmid, 1998); those species with a major degree of limb reduction show more elongated trunks and an increased number of presacral vertebrae (Presch, 1975). *Bachia bicolor* (Cope, 1896) is found in northern and central Colombia, and in western Venezuela. These lizards have an elongated trunk and tail, forelimbs with four digits, and hindlimbs reduced to the stylopodium; the body and head are narrow, and the external ear openings are absent (Dixon, 1973; Presch, 1975). Among the 17 species of the genus, *B. bicolor* shows an intermediate degree of limb reduction (Dixon, 1973; Presch, 1975; Kizirian & McDiarmid, 1998). Thus, it represents an interesting species for analysis of morphological features and their ontogenetic basis.

Information about skull morphology in *Bachia* has focused on adult forms (MacLean, 1974; Presch, 1980; Soares, 2000); therefore, detailed developmental studies would allow the recognition of morphological variation during ontogeny and adult character states. Also, the identification of structures with heterochronic patterns during ontogeny is an important tool in the determination of the potential structural constraints in *B. bicolor* skull morphology.

Here we present a detailed description of the cranial morphology in adult individuals of *B. bicolor*, and its variation during postembryonic development. As most of the evolutionary hypotheses leading to the origin of the serpentiform body plan state that cranial modifications occur in a modular form, and are subsequent to those related to the trunk and limbs (Rieppel, 1996), we focus on finding cranial traits that may indicate changes in the structural skull design, which may reveal modifications beyond those observed in the postcranial skeleton.

MATERIAL AND METHODS

All the specimens used in the study were obtained from the Colección Herpetológica of the Museo de Historia Natural, Universidad Industrial de Santander (UIS-R). Lizards were collected in the gardens of Bucaramanga City (Santander, Colombia, 07°07′28.7″N, 73°06′41.6″W, 1040-m a.s.l. altitude), fixed in 10% formalin, and stored in 70% ethanol. Thirty-eight adults and juvenile individuals of *B. bicolor* were selected; two of the juveniles hatched in the laboratory. A size series according to the snout–vent length (SVL) was established, with four stages ranging from 25.48 to 71.39 mm. Gender and sexual maturity were determined by macroscopic observation of the gonads (Appendix). The skeletal material was prepared by two methods: (1) dry skulls (six adult skulls), four of which were disarticulated, and (2) cleared and double-stained specimens, following the protocol of Wassersug (1976). The specimens were examined through an Olympus stereo microscope, and the photographs and drawings were made with the assistance of a digital camera. The cranial osteology of the dermatocranium and the otico-occipital regions was described in detail for each bone. The most significant events in the variation of the skull morphology during postnatal development were described. The anatomical terminology used herein follows Oelrich (1956), Bellairs & Kamal (1981), and Bell, Evans & Maisano (2003).

RESULTS

SKULL

The adult skull of *B. bicolor* (Fig. 1) is typical of tetrapod lizard skulls, and is very similar to that of other gymnophthalmids (MacLean, 1974; Montero, Moro & Abdala, 2002; Bell *et al*., 2003). It is between 7 and 8 mm in length, corresponding to nearly 12% of the body length (SVL). Intraspecific variation resulting from sexual dimorphism was not observed. The preorbital region is short, ending anteriorly in a slightly rounded snout. The orbits are small. The supratemporal fossa is open and bordered by a complete supratemporal arch. The otico-occipital region is very large in comparison to the rest of the skull, reaching the level of the skull table, closing the posttemporal fossa, and posteriorly protruding from the skull. The middle ear is modified, showing an extremely reduced extracolumella and a short stapes with a huge oval foot plate. The skull shows a secondary palate and a small suborbital fenestra. The hyoid apparatus is formed by a processus lingualis separated from the basihyal, hyoid cornus, small epihyals, and first ceratobranchials (Fig. 2).

The following osteological description was listed according to the location of each bone in the nasal, skull roof, temporal, orbital, palate, otico-occipital, and mandible regions.

NASAL REGION

Premaxilla: The premaxilla limits the dorsomedial rim of the nares and extends posterodorsally up to the frontal bone. The nasal process of the premaxilla overlaps posteriorly the frontal, and laterally the nasals. It has a ventral alveolar region, which bears between seven and nine unicuspid pleurodont teeth. Dorsally, the premaxilla shows a nasal process that is narrower posteriorly and wider anteriorly, but narrows between the nares (Fig. 3B). Above the nares, a small lateral process arises from the lateral border of the nasal process. Laterally, the base of the premaxilla has a maxillary process that is continuous with the alveolar region. In the ventral face of the

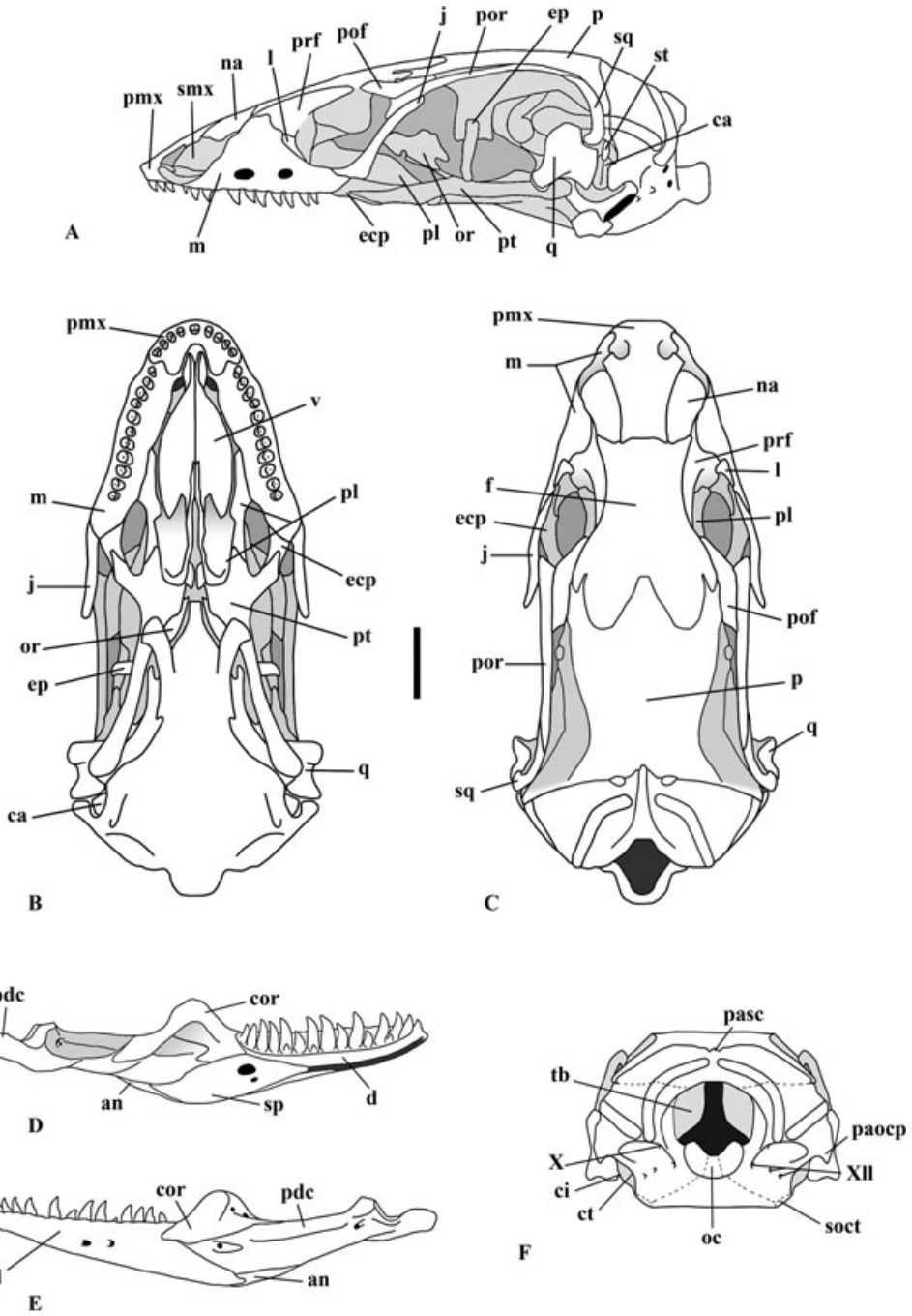

Figure 1. Adult skull and mandible of *Bachia bicolor* (UIS-R-1459). A, skull, lateral view. B, skull, palatal view. C, skull, dorsal view. D, left mandible, lingual view. E, left mandible, labial view. F, skull, posterior view. Dashed lines in (F) indicate the sutures between the neurocranial elements. Key: an, angular; ca, columella; ci, crista interfenestralis; cor, coronoid; ct, crista tuberalis; d, dentary; ecp, ectopterygoid; ep, epipterygoid; f, frontal; j, jugal; l, lacrimal; m, maxilla; na, nasal; oc, occipital condyle; or, orbitosphenoid; p, parietal; paocp, paroccipital process; pasc, supraoccipital processus ascendens; pdc, postdentary compound bone; pl, palatine; pmx, premaxilla; pof, postfrontal; por, postorbital; prf, prefrontal; pt, pterygoid; q, quadrate; soct, spheno-occipital tubercle; smx, septomaxilla; sp, splenial; sq, squamosal; st, supratemporal; tb, tympanic bulla; v, vomer; X, vagal foramen; XII, hypoglossal foramina. Scale bar = 1 mm.

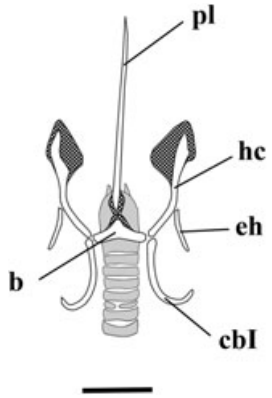

Figure 2. The hyoid apparatus of *Bachia bicolor*. Dotted areas denote cartilage. Key: b, basihyal; cbI, first ceratobranchial; eh, epihyal; hc, hyoid cornus; pl, processus lingualis. Scale bar = 1 mm.

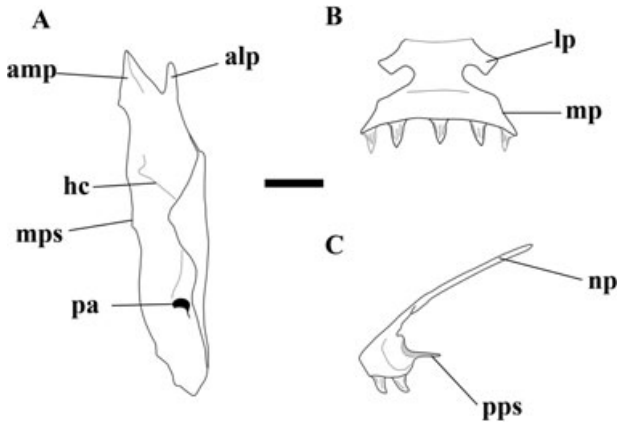

Figure 3. Maxilla and premaxilla. A, maxilla, dorsal view. B, premaxilla, anterior view. C, premaxilla, lateral view. Key: amp, anteromedial process; alp, anterolateral process; hc, horizontal crest; lp, lateral process; mp, maxillary process; mps, maxillary palatal shelf; np, nasal process; pa, posterior alveolar foramen; pps, premaxillary palatal shelf. Scale bar = 0.5 mm.

premaxilla a pair of palatal shelves extends separated by a medial slit (Figs 1B, 3C). The premaxilla meets the maxilla at the maxillary process and the palatal shelf of each side. The cartilaginous rostral tip of the septum nasale is exposed between the palatal shelf and the posteriorly placed vomers.

Nasal: Most of the dorsal margin of the nares is formed by the nasal. The nasal is a roughly rectangular element, slightly wider in its anterior portion. Each nasal is separated from its opposite in the midline by the nasal process of the premaxilla (Fig. 1A). The medial border of the nasal has a shelf, dorsally covered by the premaxilla (Fig. 4). The posterior border and most of the medial border of each nasal meet the frontal; however, the contact of the nasal medial shelf with the frontal is obscured in dorsal view by the overlapping premaxilla (Fig. 4). The nasal laterally contacts the maxilla.

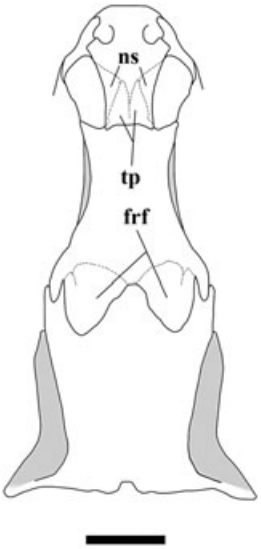

Figure 4. Overlapped surfaces of nasal, frontal, and parietal in dorsal view, denoted by dashed lines. Key: frf, frontal facets on the parietal; ns, nasal shelves; tp, triangular processes. Scale bar = 1 mm.

Maxilla: The maxilla is a triradiate element; it forms the posterolateral and ventral margins of the nares, the ventral margin of the orbit, and the lateral margin of the fenestra for Jacobson's organ. Ventrally, it has an alveolar region that bears either 11 or 12 unicuspid pleurodont teeth. There are three large processes: the premaxillary (anterior), the facial (dorsal), and the orbital (posterior) process. Medially, there is a palatal shelf that is continuous with the alveolar region, beginning at the premaxillary process and ending at the orbital process (Fig. 1B). On the palatal shelf, close to the base of the facial process, a horizontal crest is present where the lateral process of the septomaxilla dorsally rests (Fig. 3A).

At the anterior end of the maxilla, the premaxillary process bifurcates to a short and slender anterolateral process that slightly bends dorsally, and into a larger and wider anteromedial process (Fig. 3A). Both processes overlap the premaxilla, the anterolateral process overlaps the maxillary process, and the anteromedial process overlaps dorsally the palatal shelf of the premaxilla. The extreme of the anteromedial process touches the anterior process of the vomer. The facial process of the maxilla meets the nasal at its anterior margin, posteriorly overlaps the prefrontal, and contacts the lacrimal at its junction with the

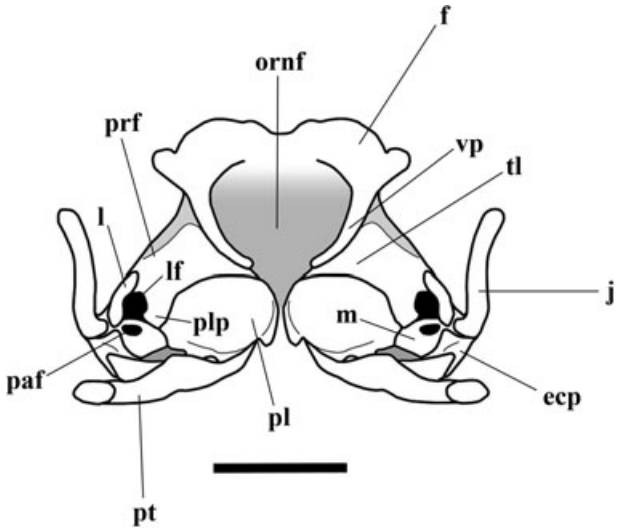

Figure 5. Posterior view of the region anterior to the orbit in a partially disarticulated skull. Key: ecp, ectopterygoid; f, frontal; j, jugal; l, lacrimal; lf, lacrimal foramen; m, maxilla; ornf, orbitonasal fenestra; paf, maxillary posterior alveolar foramen; pl, palatine; plp, prefrontal palatine process; prf, prefrontal; pt, pterygoid; tl, transverse lamina; vp, frontal ventral process. Scale bar = 1 mm.

orbital process. The maxilla contacts the palatine on the palatal shelf; posterior to that contact the maxilla forms the anterior margin of the suborbital fenestra (Fig. 1B). The posterior end of the orbital process of the maxilla is joined medially to the ectopterygoid, and dorsally to the jugal. The maxilla is pierced by the alveolar canal, which anteriorly opens at the premaxillary process and posteriorly opens at the orbital process. The lateral surface of the maxilla is perforated by several labial foramina (between one and four), with intraspecific variation and often with a bilaterally asymmetric pattern.

Skull roof

Frontals: The anterior region of the skull roof is formed by the frontals, which are fused without an evident midline suture. There are two short anterolateral and two triangular medial processes, the latter are divided by a slit (Fig. 4). The lateral margins descend and form the ventral processes that are slightly curved, without contacting at the midline (Fig. 5). Two small posterolateral processes and two large and rounded posteromedial processes (parietal tabs) are projected in its posterior margin. Posteriorly, the frontal contacts the parietal through a complex W-shaped frontoparietal suture; here, the posteromedial processes overlap the parietal, and the posterolateral processes laterally underlie the parietal (Fig. 4); this complex suture would prevent cranial mesokinesis as in other gymnophtalmids (Bell *et al*., 2003). Anteriorly, the frontal contacts the nasals laterally and the premaxilla medially. The premaxilla overlaps the medial triangular processes, which are not visible in articulated skulls (Fig. 4), whereas the short anterolateral processes lie between the nasals and the prefrontals. The frontal contacts the prefrontal along its lateral border, from the anterior corner to the base of the ventral process. The ventral process also contacts the medial portion of the prefrontal, along its anterior and ventral margin (Fig. 1A). The orbitotemporal cartilage, the planum supraseptale, extends between the extremes of the ventral processes; therefore, the olfactory peduncles are enclosed by the planum supraseptale and the frontal.

Parietal: The azygous parietal is roughly rectangular in dorsal view. Its posterior margin contacts the otico-occipital region completely closing the post-temporal fossa (Fig. 1F). The lateral descending processes of the parietal form a lateral wall, which partially closes the braincase and posteriorly contacts the alar process of the prootic (Fig. 1A). Laterally, the descending process is in slight contact with the epipterygoid. The anterior border of the parietal shows an anterolateral process that covers the posterolateral process of the frontal. At the posterior border of the parietal the supratemporal processes project in a ventrolateral direction, and the parietal fossa is found between them. A ventral crest extends throughout the base of each supratemporal process, from the parietal fossa in an anterolateral direction to the base of the descending process. The parietal attaches to the otico-occipital region by connective tissue along the ventral crest, and in the ventral surface of the supratemporal process, which overlaps the supraoccipital and partially overlaps the prootic. The posterior parietal border articulates with the otico-occipital region by the cartilaginous ascending process of the synotic tectum.

Temporal region

Postfrontal: The temporal region, located between the orbit and the otico-occipital region, shows the postfrontal that forms the posterodorsal margin of the orbit and the anterior limit of the supratemporal fossa. It is flat, slightly arched, and embraces laterally the frontoparietal suture (Fig. 1C). The lateral margin of the postfrontal joins syndesmotically with the postorbital, and in its medial margin contacts the frontal and parietal.

Postorbital: The lateral border of the supratemporal fossa is formed by the postorbital, which also forms part of the posterodorsal margin of the orbit. It is an

elongate bone, and is slender and almost straight but with a slight curvature. Its anterior end is slightly expanded and the posterior end is acute (Fig. 1C). Laterally, the postorbital joins at its anterior extreme with the jugal by syndesmosis, and its posterior extreme rests on the squamosal.

Squamosal: the posterior region of the supratemporal arch is formed by the squamosal, which borders the posterior and lateral region of the supratemporal fossa. It is a laminar bone, and is elongated and bends ventrally posteriorly (Fig. 1A). Its anterior process is acute and joins the postorbital. It joins with the supratemporal by syndesmosis, and articulates ventrally with the quadrate.

Quadrate: The quadrate is placed in ventral position with respect to the squamosal; it shows a slight lateral concavity, a gentle pronounced tympanic crest, a broad cephalic condyle, and a narrow mandibular condyle (Fig. 1A). It also has two crests: one posterior and one medial. The articulation with the squamosal lies at a dorsally placed notch, which is anterior to the cephalic condyle. The cephalic condyle articulates with the paroccipital process posteriorly and is very close to the columella (Fig. 1A, B). The mandibular condyle is involved with the ventral mandible articulation. The quadrate articulates with the pterygiod bone medially, near the mandibular condyle (Fig. 1B).

Supratemporal: The small, oval-shaped, supratemporal lies between the squamosal, cephalic condyle of the quadrate, and the paroccipital process of the otico-occipital region (Fig. 1A). Connective tissue unites it with the squamosal and quadrate.

Epipterygoid: Between the pterygoid and the parietal lies the epipterygoid in a vertical position. It is a cylindrical element that does not reach the skull roof at its dorsal tip. Ventrally, it articulates with the pterygoid by a condylar extreme. The dorsal tip touches the descending process of the parietal bone laterally (Fig. 1A).

Orbital region

Prefrontal: Each prefrontal shows a broad ventral region and a slender dorsal region that tapers, forming the supraorbital process; medially, the prefrontal shows a transverse lamina that forms the posterior wall of the nasal cavity (Fig. 5). The medial border of the prefrontal together with the palatine and the frontal limits the orbitonasal fenestra (Fig. 5). Two processes arise from the transverse lamina: the palatine process at the ventromedial corner, and another process at the dorsomedial corner that is posteriorly directed. The palatine process forms the medial margin of the lacrimal foramen (Fig. 5). The prefrontal is in tight contact with the frontal. Dorsally it reaches the anterolateral border of the frontal, and medially the transverse lamina meets the anterior and the ventral borders of the frontal ventral process. Between the palatine process and the dorsomedial processes of the prefrontal there is a contact with the convex anterior border of the palatine (Fig. 5). Anteriorly, the prefrontal meets the maxilla ventrally and the nasal dorsally. Posterolaterally, the prefrontal shows a small notch into which the lacrimal fits.

Lacrimal: The lacrimal is a small element that is broader at its anterior tip and bordering the anteroventral orbital margin. It limits the lateral rim of the lacrimal foramen and, at its anterior extreme, joins with the prefrontal, and joins ventrally with the maxilla (Fig. 5).

Jugal: The posterior and ventral borders of the orbit are formed by the jugal. It is a sigmoidal bone that is ventrally expanded at its maxillary process and tapers posteriorly towards the temporal process (Fig. 1A). The jugal touches the maxilla and the ectopterygoid at the maxillary process, whereas the temporal process joins syndesmotically with the postorbital bone.

Palatal region

Vomers: The vomers contact each other along the midline. Each vomer is narrow anteriorly and extends posteriorly, but less than the maxilla in palatal view (Fig. 1B). The lateral margin of the vomer, the maxillary palatal shelf, and the palatine maxillary process close the fenestra exochoanalis, forming a secondary palate (*sensu* Presch, 1976); therefore, the choana is opened posteriorly on the palatine (Fig. 1B).

Anteriorly, the vomer forms the medial border of the fenestra for Jacobson's organ. The vomer has two processes at its anterior tip: the anterior process, which laterally contacts the maxillary anteromedial process, and the anterolateral process that rests slightly on the maxillary palatal shelf, and which is grooved ventrally by the lacrimal groove (Fig. 6A). Ventrally, underlying the anterolateral process of the vomer is the ventral crest, and dorsal to it the medial border rises in a dorsal crest (Fig. 6A, B). On the dorsal surface of the vomer there is a transverse flange, which is posterior and very close to the dorsal crest (Fig. 6A, B). The cavity for Jacobson's organ is enclosed by the dorsal crest, the transversal flange, and the septomaxilla (Fig. 6C, D). The vomer projects posteriorly in the posterolateral and posteromedial

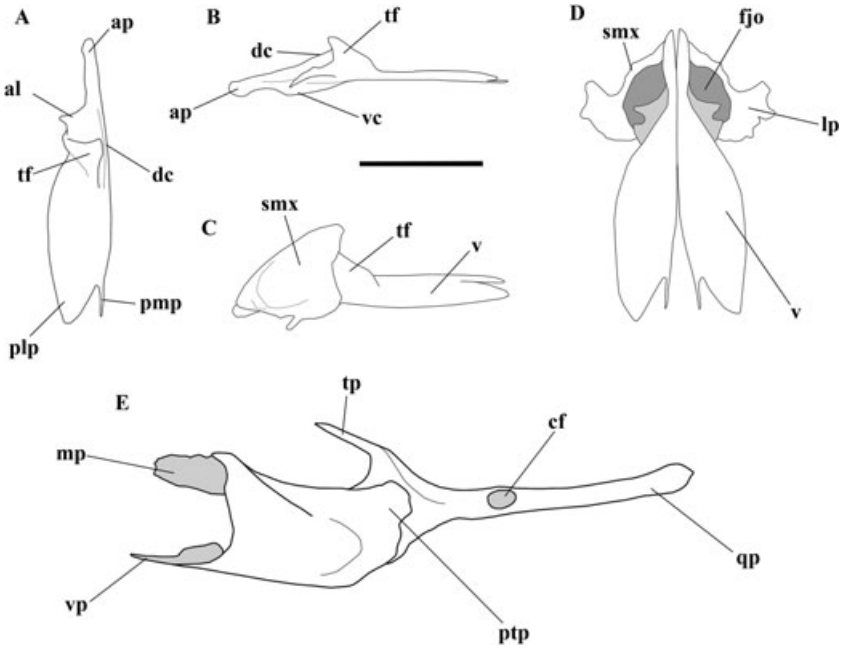

Figure 6. Palatal bones. A, vomer, dorsal view. B, vomer, lateral view. C, articulated vomer and septomaxilla in lateral view. D, articulated vomer and septomaxilla in ventral view. E, articulated palatine and pterygoid in dorsal view. Key: ap, anterior process; al, anterolateral process; cf, columellar fossa; dc, dorsal crest; fjo, fenestra for the Jacobson's organ; lp, lateral process; mp, maxillary process; plp, posterolateral process; pmp, posteromedial process; ptp, pterigoid process; qp, quadrate process; smx, septomaxilla; tf, transverse flange; tp, transverse process; v, vomer; vc, ventral crest; vp, vomerine process. Scale bar = 1 mm.

processes. The posteromedial process is short and narrow, and reaches the palatine.

Septomaxilla: Dorsal to the anterior part of the vomer is the concave septomaxilla, which forms the roof of the cavity for Jacobson's organ (Fig. 6C, D). The septomaxilla has a flat lateral process with irregular borders that rests on the maxillary palatal shelf. Ventrally, the septomaxilla covers the laterodorsal border of the vomerine transversal flange.

Palatine: The palatine ventral surface is concave, forming the palatal groove, although it is gradually less grooved posteriorly. It has two anterior processes: a narrow vomerine process, and a broad maxillary process. Posteriorly, there is an expanded pterygoid process (Fig. 6E). The vomerine process is laterally sutured to the vomer and contacts medially the contralateral palatine, the maxillary process dorsally overlaps the maxillary palatal shelf, and the pterygoid process rests on the dorsal surface of the pterygoid bone. Dorsally, the anterior border of the palatine bone, between the vomerine and the maxillary process, contacts the medial portion of the prefrontal placed dorsal to the palatine (Fig. 5). The posterolateral border of the palatine limits the suborbital fenestra medially.

Ectopterygoid: The lateral border of the suborbital fenestra is formed by the ectopterygoid (Fig. 1B). It is a laminar bone with an anterior maxillary process contacting to the maxilla, and a posteromedial process contacting the pterygoid. Dorsally, the ectopterygoid contacts the jugal.

Pterygoid: The pterygoid forms the posterior border of the suborbital fenestra. It has two anterior processes: the broad medial palatine process that overlaps ventrally the palatine, and a transverse process, which is acute and overlaps the ectopterygoid laterally. Posteriorly, the pterygoid has a quadrate process, which at its posterior end articulates laterally with the quadrate. On the dorsal surface the pterygoid exhibits the columellar fossa for the articulation of the epipterygoid (Fig. 6E). Medially, at the base of the quadrate process, the pterygoid articulates with the basipterygoid process of the basisphenoid.

Otico-occipital region

Basisphenoid: The basisphenoid is wide posteriorly and narrow anteriorly (Fig. 7A, B), and shows a smooth internal surface that is slightly concave. The posterior edge of the basisphenoid raises in a weak crista sellaris, and as a consequence it has a shallow

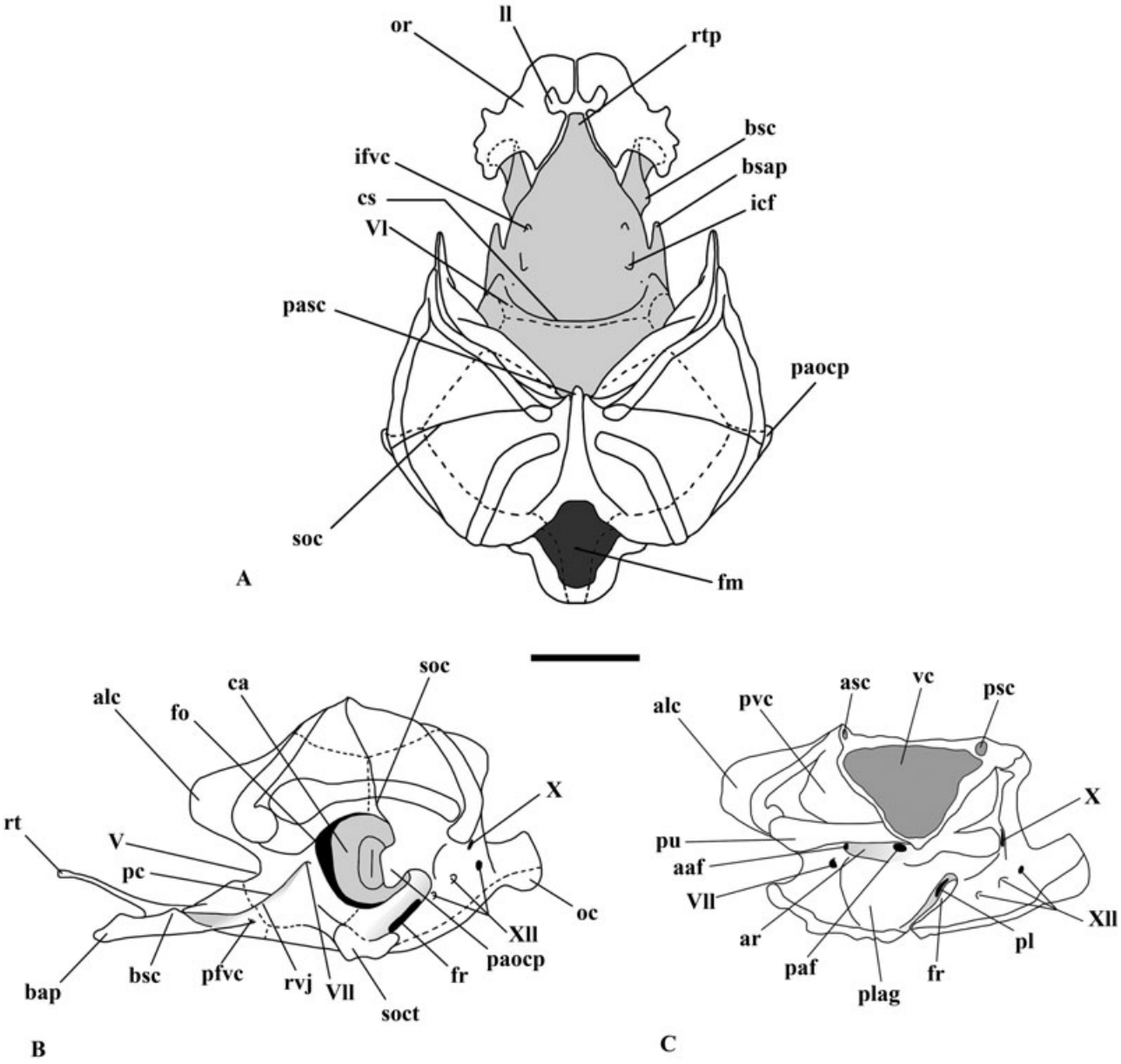

Figure 7. Adult otico-occipital region, from partially disarticulated skulls. A, dorsal view (UIS-R-1446). B, lateral view (UIS-R-1446). C, internal view (UIS-R-1448), the right prootic and the otooccipital are visible. Dashed lines indicate the sutures between the neurocranial elements in (A) and (B), and the hidden basipterygoid extremes in (A). Key: aaf, anterior auditory foramen; alc, alar crest; asc, anterior semicircular canal; ar, acoustic recess; bap, basipterygoid process; basap, basisphenoid anterior process; bsc, basisphenoid dorsal crest; ca, columella; cs, crista sellaris; fm, foramen magnum; fo, foramen ovale; fr, foramen rotundum; II, optic notch; icf, internal carotid artery foramen; ifvc, internal foramen for the vidian canal; oc, occipital condyle; or, orbitosphenoid; paf, posterior auditory foramen; paocp, paroccipital process; pasc, supraoccipital processus ascendens; pc, prootic crest; pfvc, posterior foramen for the vidian canal; pl, perilymphatic foramen; plag, prominence for the lagenar cavity; psc, posterior semicircular canal; pu, prominence of the utricule; pvc, prominence of the vestibular cavity; rt, rostral processes; rtp, rostral process; rvj, recessus vena jugularis; soc, supraoccipital transversal crest; soct, spheno-occipital tubercle; V, trigeminal notch; vc, vestibular cavity; VI, foramen for abducens; VII, facial foramen; X, vagal foramen; XII, hypoglossal foramina. Scale bar = 1 mm.

dorsum sella. Laterally and posteriorly, a stout, triangular, and anterolateraly directed alar process arises. The anterior portion of the crista prootica lies along the lateral surface of the alar process, and terminates in a small anterior process on the lateral border of the basisphenoid. Anteriorly, the basisphenoid rises dorsally forming a slender rostral process, which shows a smooth dorsal surface without crista trabecularis (Fig. 7A). The basipterygoid processes arise in the ventrolateral margins of the basisphenoid, they are widely separated, anterolaterally directed, and they have an almost horizontal position (Fig. 7B). Each basipterygoid process is crossed by two crests: a ventrolateral crest, which extends and reaches the exterior opening of the posterior foramen of the vidian canal; the other crest rises on the dorsal face of the basipterygoid process (Fig. 7A, B). The recessus vena jugularis lies between the ventrolateral crest and the crista prootica. The basisphenoid is pierced by four foramina belonging to the vidian canal. The posterior foramen is found near the suture with the prootic; it communicates internally with the carotid foramen in the base of the alar process. In front of the carotid foramen the basisphenoid shows another foramen in which the vidian canal continues; finally, the vidian canal ends in a medial foramen at the base of the basipterygoid process. The openings for the abducens canal are found posterior to the crista sellaris and anteriorly in the base of the alar process. The basisphenoid is fused with the basioccipital posteriorly and with the prootic dorsally at the posterior margin of the alar process. The anterior tip of the rostral process is continuous with the cartilage trabecula communis. The parasphenoid process is absent; however, the dermatocranial parasphenoid element probably floors the braincase ventral to the basisphenoid. The anterolateral margin of the rostral process is very close to the ventral border of the orbitosphenoid bone (Figs 1B, 7A). The basisphenoid articulates with the pterygoid by means of the anterior tips of the basipterygoid process in the palatobasal articulation.

The anteroventral limit of the braincase is formed by the orbitosphenoid (Figs 7A, 12): it is a broad and laminar element, very close to its opposite, and shows a tilted position in a similar angle as the rostral process of the basisphenoid. Its medial margin is interrupted by a large notch for the optic foramen. The lateral margin is irregular and is attached to short cartilaginous orbitotemporal remnants. In front of the medial notch the orbitosphenoid attaches to the posterior region of the orbotitemporal cartilage, the planum supraseptale.

Prootic: The prootic forms the anterior part of the otic capsule (Fig. 7A–C); it is mainly shaped by the osseous labyrinth. The prootic shows a bulked dorsal region, which encloses the vestibular cavity, and a ventral region that encloses the lagenar cavity. A constriction is present between the vestibular and lagenar cavities, and is formed at its front by the trigeminal notch and posteriorly by the foramen ovale. The prootic extends posteriorly as far as the foramen ovale. The alar process forms the lateral wall of the braincase together with the parietal, and the inferior process lies ventrally to the alar process. On the lateral surface of the prootic some structures are evident: the prominences of the anterior and horizontal semicircular canals, and its ampular recess, as well as the prominence of the lagenar recess ventrally (Fig. 7B, C). The crista prootica can be seen in the ventral region of the prootic: it begins at the basisphenoid, continues on the inferior process of the prootic, and ends at the facial foramen. The latter is close to the foramen ovale and at the same level as the trigeminal notch (Fig. 7B). The recessus vena jugularis lies below the crista prootica and continues in the basisphenoid bone. On the internal surface at the same level as the trigeminal notch, the utricular prominence is observed as a wide horizontal ridge. Ventral to the utricular prominence and anterior to the prominence of the lagenar recess, the acoustic recess is present with two foramina: the posterior auditory foramen and the anterior auditory foramen. The internal facial foramen is positioned anteroventrally relative to the acoustic recess (Fig. 7C). The prootic shows synostotic unions with the basisphenoid anteriorly, with the otooccipital and the basioccipital posteriorly, and with the supraoccipital dorsally.

Otooccipital: The otooccipital forms the posterior part of the otic capsule (Fig. 7A–C). Similar to the prootic, the otooccipital enclose a large dorsal vestibular cavity and a ventral lagenar cavity. The otooccipitals form the lateral portions of the occipital condyle, and the basioccipital lies between them. Laterally, each otooccipital borders the foramen magnum. Anteriorly, the otooccipital forms the posterior margin of the foramen ovale; the short and anteriorly directed paroccipital process lies behind the foramen ovale. On its lateral face, the otooccipital shows the prominences of the horizontal and posterior semicircular canals, and the prominence of the posterior ampullar recess (Fig. 7B). The jugular recess is found below the prominence of the posterior ampullar recess, where the exterior vagus foramen opens; ventral to the vagus foramen, three hypoglossal foramina are present orientated in anteroventral direction. Internally, posterior to the prominence of the vestibule (tympanic bulla), the internal vagus foramen is found; below it there are three internal hypoglossal foramina. The perilymphatic foramen is located in the backside of the prominence of the lagenar recess

(opening into the lagenar cavity), and the internal opening of the foramen rotundum is present in close proximity (Fig. 7C). There is a deep occipital recess, which opens in a narrow and elongated (slit-like) foramen rotundum with a tilted position (Fig. 7B). The occipital recess is posteriorly limited by the crista tuberalis, which arises at the base of the paroccipital process and reaches the anteroventral margin of the otooccipital at the spheno-occipital tubercle. The crista interfenestralis also arises at the base of the paroccipital process; it forms the posteroventral margin of the foramen ovale, reaches the spheno-occipital tubercle, and limits the occipital recess anteriorly. In posterior view, the crista interfenestralis and the crista tuberalis are not at the same level, because the crista interfenestralis is more pronounced with respect to the crista tuberalis (Fig. 1F).

Supraoccipital: The supraoccipital extends between the otic capsules (Fig. 7A, B), forms the dorsal closure of the neurocranium, enclosing the otic capsule, and borders the foramen magnum dorsally. In the midline, the supraoccipital shows a constriction that separates the vestibular cavities of each side. The supraoccipital has a small processus ascendens of the synotic tectum anteriorly, with a slightly calcified cartilaginous tip. The supraoccipital shows a depression on the midline between the vestibular cavities, extending between the foramen magnum and the processus ascendens; the prominences of the anterior and posterior semicircular canals are also observed on the dorsal surface. The supraoccipital is crossed by a transversal crest dorsally, which arises above the paroccipital process of the otooccipital, parallel to the otooccipital-prootic suture, reaching the processus ascendens (Fig. 7A, B). The tympanic bullae bulge ventral to the supraoccipital; each is pierced by the endolymphatic foramen. Ventrally, the supraoccipital is fused with the prootic anteriorly and with the otooccipital posteriorly. It is sutured to the parietal anterior to the transversal crest. The cartilaginous tip of the processus ascendens fits into the parietal fossa.

Basioccipital: The braincase floor is formed mainly by the basioccipital (Fig. 7A, B); it is pentagonal-shaped, with a long and slender posterior apex, which is dorsally curved and forms part of the occipital condyle. Its ventral and dorsal surfaces are smooth, with the dorsal one being slightly concave. It fuses with the basisphenoid anteriorly, with the prootic anterolaterally, and with the otooccipital posterolaterally. At the point where the basioccipital, the prootic, and the otooccipital meet, the spheno-occipital tubercle is found, which forms the ventral margins of the occipital recess and the foramen rotundum (Fig. 7B).

Columella: The columella is very short, its shaft is nodular shaped, and it has a huge foot plate (Fig. 7B), laterally it bears an extremely reduced extracolumella. The columella is positioned very close to the paroccipital process posteriorly and to the cephalic condyle of the quadrate anteriorly.

MANDIBLE

Dentary: The dentary is crossed by Meckel's canal, which is posteriorly closed by the splenial, but is open at the anterior extreme, where Meckel's cartilage is visible (Fig. 1D). The alveolar region of the dentary bears between 13 and 15 unicuspid pleurodont teeth. The dentary articulates with its opposite at its anterior end, in the mandibular symphysis. The dentary contacts the coronoid dorsally, and covers the postdentary compound bone in labial view and the angular ventrally.

Angular: The angular is positioned posterior to the dentary; it is small and forms the ventrolateral angle of the mandible (Fig. 1E).

Splenial: The splenial is visible in lingual view (Fig. 1D). It is oval shaped with sharp extremes, and partially closes Meckel's canal. Posteriorly, the splenial contacts the postdentary compound bone and the angular, dorsally and ventrally, respectively. Two anterior foramina are present: the large and dorsal alveolar foramen, and the small and ventral mylohyod foramen.

Coronoid: The coronoid lies dorsally and forms the coronoid process. It is rounded and has three processes: the posteromedial, the anteromedial, and the anterolateral process (Fig. 1D, E). The coronoid lies dorsal to the postdentary compound bone and the splenial; it contacts the dentary anteriorly and also contacts the dentary with its anterolateral process.

Postdentary compound bone: The posterior half portion of Meckel's canal is formed by a postdentary compound bone product of the postnatal fusion of the articular and surangular, and has a large adductor fossa (Figs 1D, E, 8D, E). The articular surface of the mandible is present behind the adductor fossa, which has a tilted position. Posteriorly, there is a narrow retroarticular process. On the lingual face of the postdentary compound bone, anterior to the retroarticular process, is a slightly pronounced angular process, although it resembles a crest rather than a process (Fig. 1D). The postdentary compound bone contacts all the elements of the mandible, dorsally the

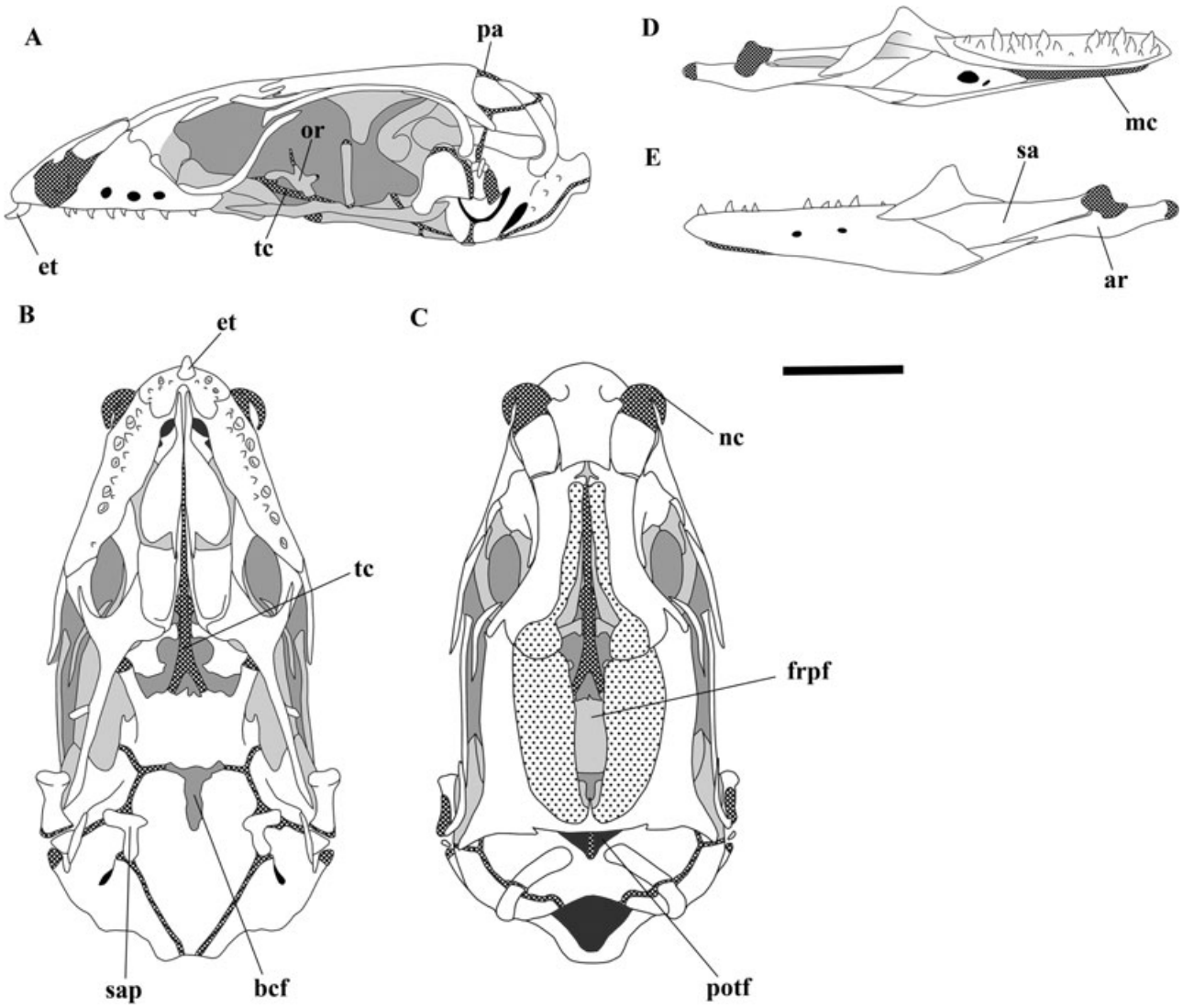

Figure 8. Neonate skull and mandible of *Bachia bicolor* (UIS-R-1452). White dotted areas denote cartilage; black dotted areas denote scattered mineralization, suggesting membranous ossification. A, skull, lateral view. B, skull, ventral view. C, skull, dorsal view. D, mandible, lingual view. E, mandible, labial view. Key: ar, articular bone; bcf, basicranial fenestra; et, egg tooth; frpf, frontoparietal fontanelle; mc, Meckel's cartilage; nc, nasal cupola; or, orbitosphenoid; pa, processus ascendens of the tectum synoyicum; potf, post-temporal fossa; sa, surangular; sap, spheno-occipital tubercle apophyseal ossification; tc, trabecula communis. Scale bar = 1 mm.

coronoid, ventrally the angular, laterally the dentary, and medially the splenial.

POSTNATAL DEVELOPMENT

NEONATES

All the bones that comprise the adult skull are present in the neonates (Fig. 8). Some of the chondrocranium and splanchnocranium components are partially ossified. The skull roof is ossified only at the posterior and lateral margins of the parietal and the lateral margins of the frontal, thus leaving a large frontoparietal fontanelle on the roof (Fig. 9A). The post-temporal fossa is open. The dorsal and ventral extremes of the epipterygoid and the quadrate bones are capped by cartilage; the articular surface and the extreme of the retroarticular process in the mandible are also covered by cartilage. There are some apophyseal ossifications: on the cephalic condyle of the quadrate, on the dorsomedial portion of the articular surface, and on the retroarticular process. The elements of the otico-occipital region are sutured synchondrotically; the extremes of the basipterygoid processes and paroccipital processes are capped by

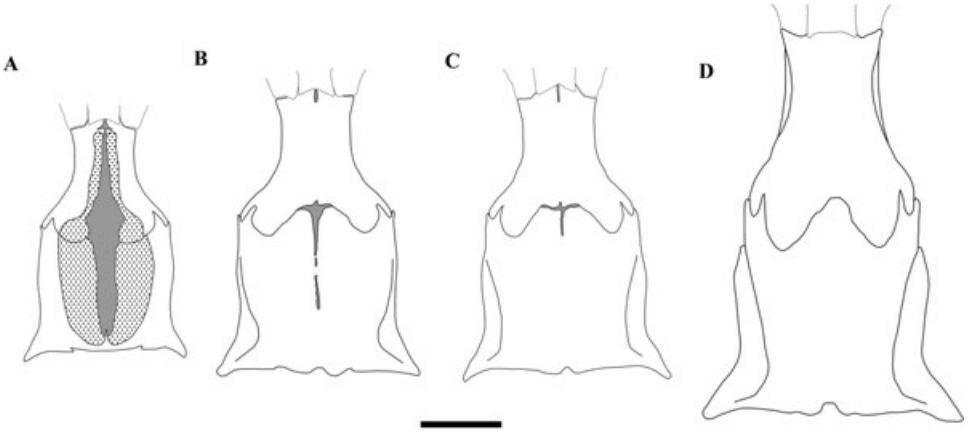

Figure 9. Progressive closure of the frontoparietal fontanelle fusion of frontals and parietals, and the differentiation of the frontoparietal suture during postnatal development. White dotted areas denote mineralization, suggesting membranous ossification in the neonate. The fontanelle is highlighted in grey. A, neonate (UIS-R-1452). B, UISR-1451. C, UISR-1245. D, full-grown adult (UIS-R-1442). Scale bar = 1 mm.

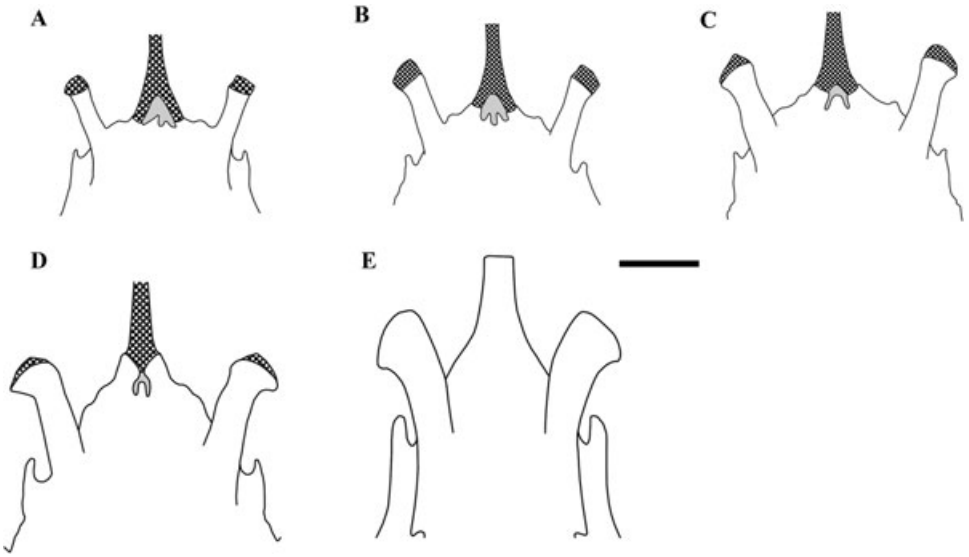

Figure 10. Progressive ossification of the trabecular cartilage and the cartilage trabecula communis, showing morphological intraspesific variation in the basisphenoid rostrum during postnatal development. Ventral view. A, neonate (UIS-R-1452). B, UIS-R-1451. C, UISR-1443. D, UISR-1437. E, full ossified adult (UIS-R-1453). Scale bar = 0.5 mm.

cartilage, and the processus ascendens of the supraoccipital is cartilaginous. The spheno-occipital tubercles are barely visible, being covered by a large apophyseal ossification (Fig. 8B). The anterior border of the basisphenoid is not well defined – it lacks the rostral process – and instead has a pituitary fossa (Figs 10, 12). Between the basisphenoid and the basioccipital there is the basicranial fenestra (Fig. 8B). The prootic lacks the alar crest, and the parietal descending processes are short and slender, leaving the lateral wall of the braincase open (Fig. 8A). The orbitosphenoid is less broad than in the adult, but it is ossified and sketches the shape and position of the adult (Figs 8A, 12). In neonates the orbitosphenoid is present as a compound bone; it has a core endochondral ossification with membranous growths around it (Fig. 11). Tables 1 and 2 summarize the most significant events in postnatal development.

DISCUSSION

The skull of *B. bicolor* shares several features with the skull of other species of *Bachia* (MacLean, 1974; Soares, 2000) and the skulls of other gymnophthalmid lizards (MacLean, 1974; Montero *et al.*, 2002; Bell *et al.*, 2003). However, the skull of *B. bicolor* also

shows convergent morphological similarities with other fossorial/burrowing serpentiform lizards. The evolution of a serpentiform body plan seems to be a frequent event, which has occurred independently within squamate lizards (Estes *et al*., 1988; Lee, 1998). Several authors point out that characters, like limb reduction, body elongation, miniaturization, and cranial modifications, would be functionally correlated as an adaptation to fossoriality (Rieppel, 1981, 1984, 1996; Lee, 1998). Rieppel (1981, 1984, 1996) states that those characters were integrated in the origin of the serpentiform body plan: the cranial skeleton was modified in parallel to the postcranial skeleton, following a trend within an adaptative scenario (burrowing habits), and ending in a serpentiform lizard with particular cranial modifications. These modifications would be associated with evolutionary processes like miniaturization, with a reduction in head and body diameter.

In the genus *Bachia*, Presch (1975; see also Dixon, 1973) claims that limb reduction, body elongation, and reduction in head and body diameter are correlated with the evolution of this group towards fossorial habits, which suggest that *B. bicolor* can be regarded as an intermediate morphotype between the saurian and the serpentiform ecomorphs. There are some shared similarities in the skull of *B. bicolor* with other species of *Bachia* (MacLean, 1974; Presch, 1980; Hoyos, 1998; Soares, 2000; Bell *et al*., 2003): preorbital shortening, descendent frontal lateral margins that do not touch each other medially, W-shaped frontoparietal suture, reduced maxillary tooth number, free lacrimal, small quadrate, small ends of the basipterygoid process, reduced columella with increased footplate size, open Meckel's canal, and an enlarged splenial. Some regions show interspecific variation: the presence of a premaxillary nasal process reaching the frontal and separating the nasals in the midline, vertical or tilted epipterygoid, and open or closed supratemporal fossa.

Bachia bicolor shares more general characters with other gymnophthalmid lizards: fused frontals, lack of pineal foramen, frontal tabs overlapping the parietal, secondary plate, and a compound postdentary element (Presch, 1976; Estes *et al*., 1988; Montero *et al*., 2002; Bell *et al*., 2003).

Bachia bicolor shows convergent cranial characters with different serpentiform lizards of the Scincidae, Amphisbaenia, Dibamidae, Serpentes and Pygopodidae (Rieppel, 1981, 1984; Greer, 1985; Lee, 1998; Montero & Gans, 1999; Rieppel & Zaher, 2000; Kearney, 2003): short preorbital region, large otico-occipital region, closed post-temporal fossa, closed lateral wall of the braincase, slit-like foramen rotundum, complex frontoparietal suture, large footplate of the columella, reduced tympanic crest of the quadrate, reduced parietal supratemporal process, short epipterygoid, broad orbitosphenoid, short and anteriorly directed paroccipital processes, an almost planar basisphenoid internal surface, very low dorsum sellae,

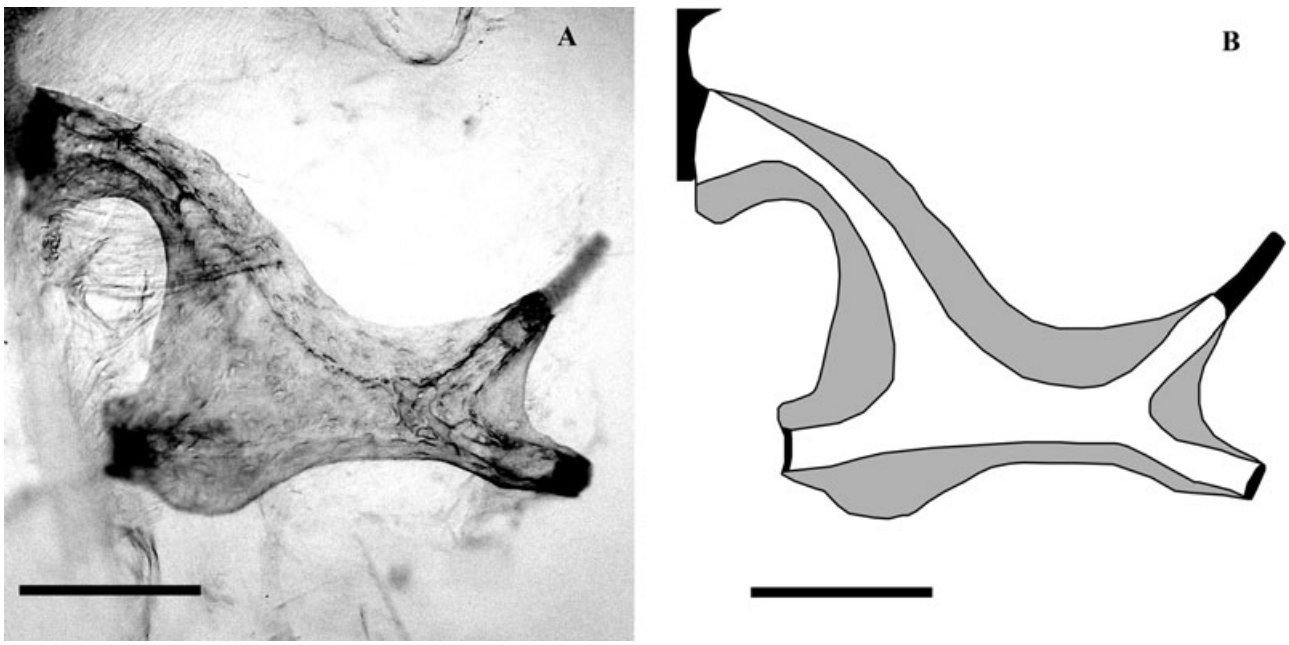

Figure 11. Right orbitosphenoid of neonate in dorsal view. Anterior to the top (UIS-R-1452). A, photograph. B, schematic drawing where cartilage is represented in black; mineralization of membranous ossifications is represented in grey, and endochondral ossification is represented in white. Scale bar = 0.25 mm.

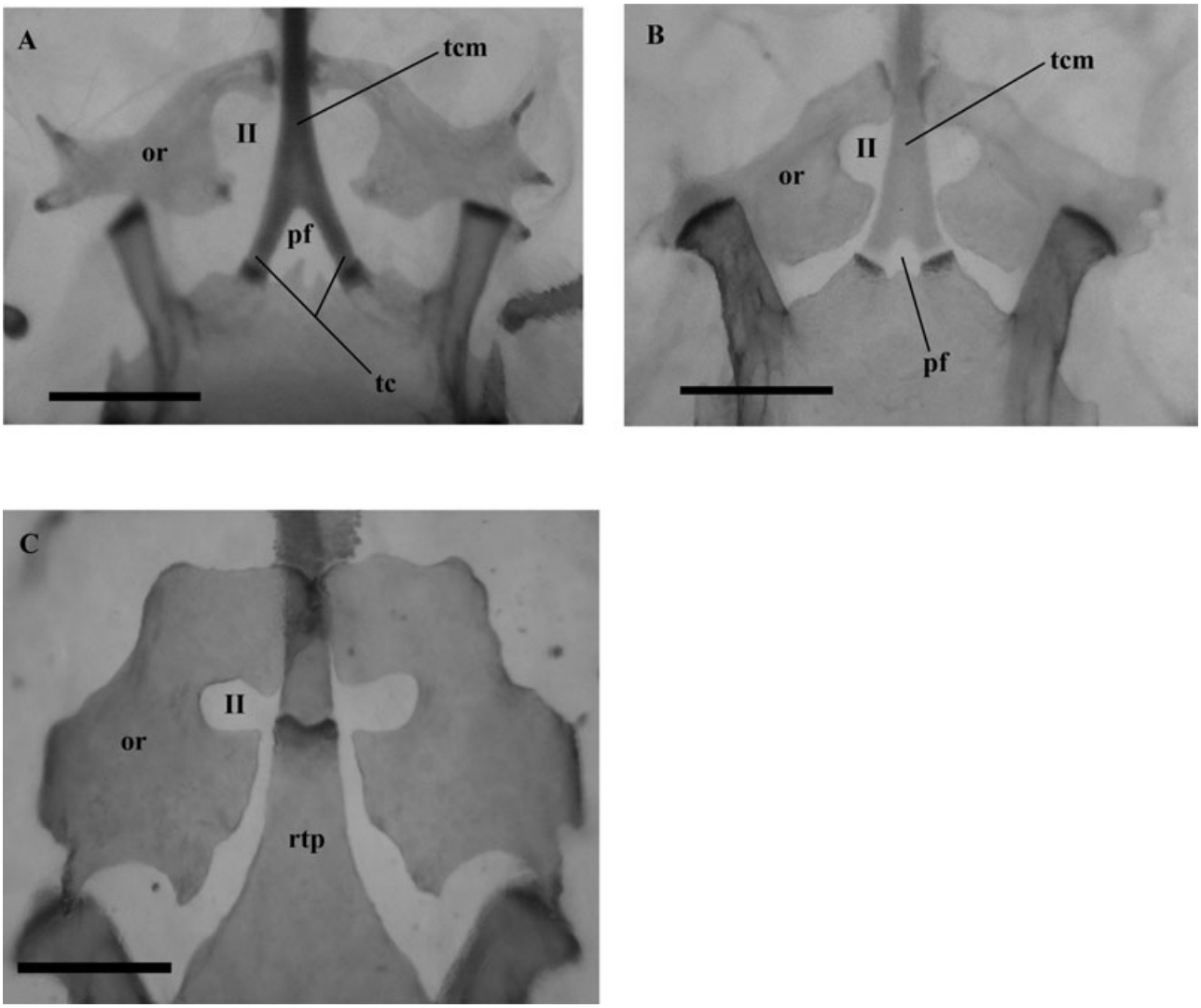

Figure 12. Anterior braincase region showing the orbitosphenoid growth, the ossification of the trabecular cartilage, and trabecula communis at different ontogenetic stages. A, neonate (ventral view, UIS-R-1452). B, juvenile (ventral view, UIS-R-1438). C, adult (dorsal view, UIS-R-1453). Key: II, optic foramen notch; or, orbitosphenoid; pf, pituitary fossa; rtp, rostral process; tc, trabecular cartilage; tcm, trabecula communis. Scale bar = 0.5 mm.

extended but barely pronounced crista sellaris, and a low interorbital septum. However, not all of these characters are present in all the serpentiform lineages listed above; moreover, some of these characters are present in nonserpentiform but miniaturized lizards.

Hence, lizards like *B. bicolor* show the coexistence of several of those body-plan modifications: body elongation, limb reduction, short snout, and enlarged skull posterior region (increased otico-occipital region relative to the dermatocranium). However, the cranial modifications of *B. bicolor* relative to most squamate lizards are discrete, as they are displayed on isolated traits, are apparently not integrated, and would seem to be related to small size. Considering that limb reduction and body elongation are evident within the genus *Bachia*, interspecific variation suggests that there is a greater flexibility in the postcranial body plan, whereas the cranial structural design is more restricted.

The skull of *B. bicolor* shows some derived morphological similarities present in particular groups within Squamata (Estes *et al*., 1988). The vidian canal is open on the basisphenoid dorsal surface, as described in Serpentes (Estes *et al*., 1988; Rieppel & Zaher, 2000), and the genera *Anelytropsis* and *Dibamus* of Dibamidae (Greer, 1985); however, the positions of the external foramina (anterior and

Table 1. The most significant events in postnatal development of the *Bachia bicolor* skull, at four stages of snout–vent length (SVL)

Elements	Neonate–40 mm	40–50 mm	50–60 mm	60–70 mm
Frontals	Fuses. Ventral process is differentiated and reaches 1/4 of its maximum extension.	Ventral process reaches half of its maximum extension.	The ventral process reaches 3/4 of its maximum extension.	The ventral process reaches its maximum extension.
Parietal	A long slit in the midline is still visible.	Ossifies completely.	Completely ossified.	Completely ossified.
Prefrontal	Posterior process reaches 1/4 of its maximum extension.	The posterior process reaches half of its maximum extension.	The posterior process reaches its maximum extension.	Together with the frontal, it completes the orbital medial wall.
Quadrate	Two defined apophyses on the tympanic crest and on the cephalic condyle.	The apophyses grow.	The apophyses grow.	The apophyses fuse.
Epipterygoids	Separated from parietals.	In lateral contact with parietal.	In lateral contact with parietal.	In lateral contact with parietal. Dorsal and ventral epiphyses fuse.
Neurocranium bones	Joined by synchondrosis.	Joined by synchondrosis.	Joined by synchondrosis.	Fused.
Basisphenoid	Trabecular cartilages ossify up to half of its length.	Trabecular cartilages ossify up to 3/4 of its length.	Trabecular cartilages ossifies completely, and fuses with its opposite medially. The dorsal crest of the basipterygoid process arises.	The *trabecula comunis* forms the rostral process. The basipterygoid processes ossifies completely.
Otooccipital	Lateral apophyses on the paroccipital process.	Lateral apophyses grow.	Ventral apophyses on the paroccipital process arise.	The apophyses fuse, the paroccipital process ossifies completely.
Prootic	The alar crest arises in front of the ampullar prominence.	The alar crest extends above the semicircular canal.	The alar crest reaches the descending process of the parietal, closing the braincase laterally.	The alar crest reaches its maximum extension.
Postdentary compound bone	Two cartilaginous apophyses (dorsomedial ands dorsolateral) on the articular surface.	The articular surface ossifies.	The articular surface ossifies completely, and the apophyses fuse.	The apophyses on the retroarticular process fuse. The surangular and articular bones fuse.

Table 2. Postnatal development of cranial spaces of *Bachia bicolor* at four stages of snout–vent length (SVL)

Cranial spaces	Neonate–40 mm	40–50 mm	50–60 mm	60–70 mm
Post-temporal fossa				
Frontoparietal fontanela	Open	Reduced	Closed	Closed
Basicranial fenestra				
Pituitary fossa	Open	Open	Reduced, ossified margins	Closed

posterior) are similar to that of other lizards (Oelrich, 1956), rather than those present in Serpentes and Dibamidae. The trabecular cartilages and a portion of the cartilage trabecula communis ossify during postnatal development, forming the basisphenoid rostral process, a condition that has only been observed in Pygopodidae (Underwood, 1957; Stephenson, 1961). The name septosphenoid has been recommended for that process (Bellairs & Kamal, 1981); however, the ossification is flat in *B. bicolor*, rather than tubular as described in Pygopodidae. The ventral surface of the spheno-occipital tubercles are capped by a broad apophysis; in adults this apophysis fuses to the otico-occiptal region, as described in Amphisbaenia (Montero & Gans, 1999; Kearney, 2003), and in the skinks *Acontias* and *Feylinia* (Rieppel, 1981).

A remarkable feature of the skull of *B. bicolor* is the orbitosphenoid bone. In most squamate lizards the orbitosphenoid is small and arch shaped, it is formed by the ossification of the orbitotemporal cartilages (taenia medialis, pila metoptica, and neighbouring regions) (Bellairs & Kamall, 1981) bordering the optic foramen posterolaterally. In *B. bicolor*, the orbitosphenoid is paired, broad, planar, in close proximity to its opposite in the midline, and shows a tilted position in an angle similar to the basisphenoid rostral process. Also, the orbitosphenoid closes the braincase anteroventrally, but it does not touch any skull element. In Amphisbaenia, the orbitosphenoid is very different from other squamates, being azygous and, like *B. bicolor*, closing the braincase anteroventrally. In contrast to *B. bicolor*, the orbitosphenoid of amphisbaenids shows a tight contact with the parabasisphenoid, frontal, and parietal (Montero & Gans, 1999; Maisano, Kearney & Rowe, 2006). The analyses of embryological material in Amphisbaenia (Bellairs & Gans, 1983; Montero, Gans & Lions, 1999) reveal that the orbitosphenoid bone is a compound bone [with chondral (of dubious identity) and membranous ossifications]: for this reason the name 'tabulosphenoid' was recommended, in view of its unique morphology and nonhomology with the orbitosphenoid bone of most squamates (Montero & Gans, 1999; Montero *et al*., 1999). On the other hand, Kritzinger (1946) described paired orbitosphenoids in the amphisbaenian *Monopeltis capensis* that are anteriorly fused and diverge posteriorly into two lateral wings. In addition, recent work based on high-resolution X-ray computed tomography revealed that in the fossil amphisbaenid *Rhineura hatcherii*, no tabulosphenoid-like element exists; instead, it shows a paired element, which is relatively broad and close to its opposite medially, and was identified by Kearney, Maisano & Rowe (2005) as the orbitosphenoid. The latter is roughly similar to the orbitosphenoids in *B. bicolor*; however, the orbitosphenoids in *R. hatcherii* are inside the braincase, enclosed by the frontals, and lack an optic foramen.

In contrast to other lizards, the orbitosphenoid of *B. bicolor* is not expanded by the ossification of the orbitotemporal cartilages during postnatal development (Bellairs & Kamall, 1981). The neonates of *B. bicolor* present an ossified orbitosphenoid, the shape and position of which are similar to the adult morphology, but it expands, nearly closing the braincase anteroventrally without the ossification of adjacent orbitotemporal cartilages during postnatal development. In neonates, the orbitosphenoid is observed as a compound element, it has the endochondral ossification of the orbitotemporal cartilages connected to the planum supraseptale, and membranous ossifications around and continuous to those cartilages, giving it a broader shape in neonates, which grows during postnatal development until it reaches the adult shape/size.

In summary, the orbitosphenoids in *B. bicolor* are broad elements that form part of the anterior braincase floor; although they are not as enlarged as in most amphisbaenians, they resemble the elements observed in *R. hatcherii* (Kearney *et al*., 2005). The orbitosphenoid in *B. bicolor* is attached to the planum supraseptale, but does not contact any other skull elements; whereas in most amphisbaenians it does, but does not attach to any orbitotemporal cartilage. The orbitosphenoid is a compound bone in *B. bicolor*, it has a chondral nucleus (attached to the planum supraseptale) with membranous growths around it, which expand during postnatal development, similar to the ontogenetic origin of this element in Amphisbaenia (Bellairs & Gans, 1983; Montero *et al*., 1999). An exhaustive analysis of orbitosphenoid variation during ontogeny within Squamata would establish the equivalence or homologies of the orbitosphenoid

components in *B. bicolor*. At the moment it can only be claimed that the orbitosphenoid in *B. bicolor* shows unique and distinctive features with respect to most Squamata, and that it is structurally comparable with the orbitosphenoid in Amphisbaenia.

Excluding the observed conditions in the orbitosphenoid and the basisphenoid rostral process, the neonatal state of ossification and the pattern of postnatal development follow the general pattern described until now in other squamates (Rieppel, 1992; Barahona & Barbadillo, 1998; Maisano, 2001): there is a large frontoparietal fontanelle on the skull roof, which ossifies towards the midline fusing the parietals and the frontals (azygous in Gymnophthalmidae; Estes *et al*., 1988; Maissano, 2001); an open basicranial fenestra in neonates; and the fusion of neurocranial elements, apophyses, and ossified secondary centres.

Some of the convergent features observed in the skull of *B. bicolor* with respect to other serpentiform lizards arise entirely during postnatal ontogeny: the lateral wall of the braincase, the closure of the posttemporal fossa, the anteroventral closure of the braincase by the expansion of the orbitosphenoid, and the ossification of the basisphenoid rostral process. Other characters showing interspecific variation within Gymnophthalmidae also arise during postnatal development (as noted by Barahona & Barbadillo, 1998 for some Lacertid lizards, and by Bell *et al*., 2003 for *Neusticurus ecpleopus*), such as the complex W-shaped frontoparietal suture and the frontal ventral process. Therefore, postnatal heterochronic changes may have an important role in the modification of cranial structural design within Gymnophthalmidae and Squamata, as mentioned by Rieppel (1993, 1996) for the origin of the ophidian skull morphology.

The data presented in this work, in relation to morphologies in postnatal development, would be significant when considering the interspecific variation related to heterochronic patterns in phylogenetic analyses of the species of *Bachia*.

The structural design of the *B. bicolor* skull has shared features with other species of *Bachia*, and also with other gymnophthalmid lizards. However, some isolated features, such as the basisphenoid rostral process only described in the serpentiform lizards of the Pygopodidae, and the compound orbitosphenoid bone (chondral and membranous), reveal important structural changes in cranial anatomy, which highlights the need for a more comprehensive taxonomic examination in an ontogenetic series of other species of *Bachia* and Gymnophthalmidae to understand the morphological changes and to interpret them in an evolutionary scenario, within a phylogenetic framework.

ACKNOWLEDGEMENTS

We thank Ricardo Montero and Maureen Kearney for providing helpful comments and criticism on early drafts of the manuscript, and Ricardo Montero and Cristina Rodriguez for improving the English. Two anonymous reviewers made suggestions and valuable comments on the manuscript. We thank Francisca Leal for processing some of the cleared and double-stained specimens, and the Laboratorio de Biología Reproductiva de Vertebrados for its support during this research. This study was partially funded by Consejo Nacional de Investigaciones Cientificas y Técnicas-Argentina (PIP 2829) and Agencia Nacional de Promoción Científica y Técnica-Argentina (PICT 12418) to MF.

REFERENCES

Barahona F, Barbadillo LJ. 1998. Inter- and intraspecific variation in the post-natal skull of some lacertid lizards. *Journal of Zoology, London* **245:** 393–405.

Bell CJ, Evans SE, Maisano JA. 2003. The skull of the gymnophthalmid lizard *Neusticurus ecpleopus* (Reptilia: Squamata). *Zoological Journal of the Linnean Society* **139:** 382–304.

Bellairs Ad'A, Gans C. 1983. A reinterpretation of the amphisbaenian orbitosphenoid. *Nature* **302:** 243–244.

Bellairs Ad'A, Kamal AM. 1981. The chondrocranium and the development of the skull in recent reptiles. In: Gans C, Parsons T, eds. *Biology of the reptilia, vol. 11. Morphology* F. New York: Academic Press, 1–263.

Dixon JR. 1973. Systematic review of the teiid lizard genus *Bachia* with remarks on *Heterodactylus* and *Anotosaura*. *University of Kansas Museum of Natural History, Miscellaneous Publications* 57, 1–47.

Estes R, de Queiroz K, Gauthier J. 1988. Phylogenetic relationships within Squamata. In: Estes R, Pregill G, eds. *Phylogenetic relationships of the lizard families*. Stanford: Stanford University Press, 119–281.

Greer AE. 1985. The relationships of the lizard genera *Anelytropsis* and *Dibamus*. *Journal of Herpetology* **19:** 116–156.

Hoyos JM. 1998. A reappraisal of the phylogeny of lizards of the family Gymnophthalmidae (Sauria, Scincomorpha). *Revista Española de Herpetología* **12:** 27–43.

Kearney M. 2003. Systematics of the Amphisbaenia (Lepidosauria: Squamata) based on morphological evidence from Recent and fossil forms. *Herpetological Monographs* **17:** 1–74.

Kearney M, Maisano JA, Rowe T. 2005. Cranial anatomy of the extinct amphisbaenian *Rhineura hatcherii* (Squamata, Amphisbaenia) based on high-resolution X-ray computed tomography. *Journal of Morphology* **264:** 1–33.

Kizirian DA, McDiarmid RW. 1998. A new species of *Bachia* (Squamata: Gymnopthalmidae) with plesiomorphic limb morphology. *Herpetologica* **54:** 245–253.

Kritzinger CC. 1946. The cranial anatomy and kinesis of the

South African amphisbaenid *Monopeltis capensis* Smith. *South African Journal of Science* **42:** 175–204.

Lee MYS. 1998. Convergent evolution and character correlation in burrowing reptiles: towards a resolution of squamate relationships. *Biological Journal of the Linnean Society* **63:** 369–453.

MacLean WP. 1974. Feeding and locomotor mechanisms of teiid lizards: functional morphology and evolution. *Papéis Avulsos de Zoologia, São Paulo* **27:** 173–213.

Maisano JA. 2001. A survey of state of ossification in neonatal squamates. *Herpetological Monographs* **15:** 135–157.

Maisano JA, Kearney M, Rowe T. 2006. Cranial anatomy of the spade-headed amphisbaenian *Diplometopon zarudnyi* (Squamata, Amphisbaenia) based on high-resolution X-ray computed tomography. *Journal of Morphology* **267:** 70–102.

Montero R, Gans C. 1999. The head skeleton of *Amphisbaena alba* Linnaeus. *Annals of the Carnegie Museum* **68:** 15–80.

Montero R, Gans C, Lions ML. 1999. Embryonic development of the skeleton of *Amphisbaena darwini heterozonata* (Squamata: Amphisbaenidae). *Journal of Morphology* **239:** 1–25.

Montero R, Moro SA, Abdala V. 2002. Cranial anatomy of *Euspondylus acutirostris* (Squamata: Gymnophthalmidae) and its placement in a modern phylogenetic hypothesis. *Russian Journal of Herpetology* **9:** 215–228.

Oelrich TM. 1956. The anatomy of the head of *Ctenosaura pectinata* (Iguanidae). *Miscellaneous Publications, Museum of Zoology, University of Michigan* **94:** 1–122.

Pellegrino KCM, Rodrigues MT, Yonenaga-Yassuda Y, Sites JW. 2001. A molecular perspective on the evolution of microteiid lizards (Squamata, Gymnophthalmidae), and a new classification for the family. *Biological Journal of the Linnean Society* **74:** 315–338.

Presch W. 1975. The evolution of limb reduction in the teiid lizard genus *Bachia*. *Bulletin Southern California Academy of Sciences* **74:** 113–121.

Presch W. 1976. Secondary palate formation in microteid lizards (Teiidae, Lacertilia). *Bulletin Southern California Academy of Sciences* **75:** 281–283.

Presch W. 1980. Evolutionary history of the South American microteiid lizards (Teiidae: Gymnophthalminae). *Copeia* **1980:** 36–56.

Rieppel O. 1981. The skull and the jaw adductor musculature in some burrowing scincomorph lizards of the genera *Acontias*, *Typhlosaurus* and *Feylinia*. *Journal of Zoology, London* **195:** 493–528.

Rieppel O. 1984. Miniaturization of the lizard skull: its functional and evolutionary implications. *Symposium of the Zoological Society London* **52:** 503–520.

Rieppel O. 1992. Studies on skeleton formation in reptiles. III. Patterns of ossification in the skeleton of *Lacerta vivipara* Jacquin (Reptilia, Squamata). *Fieldiana Zoology, New Series* **68:** 1–25.

Rieppel O. 1993. Patterns of diversity in the reptilian skull. In: Hanken J, Hall BK, eds. *The skull, vol. 2: patterns of structural and systematic diversity*. Chicago, IL: University of Chicago Press, 344–390.

Rieppel O. 1996. Miniaturization in tetrapods: consequences for skull morphology. *Symposium of the Zoological Society London* **69:** 47–61.

Rieppel O, Zaher H. 2000. The braincases of mosasaurs and *Varanus*, and the relationships of snakes. *Zoological Journal of the Linnean Society* **129:** 489–514.

Soares M. 2000. Estudo do esqueleto cefálico de *Anotosaura* Amaral, 1933, *Bachia* Gray, 1845 e *Heterodactylus* Spix, 1825 (Squamata, Teiioidea, Gymnophthalmidae). *Boletim do Museo Nacional, Nova sâerie, Zoologia* **426:** 1–20.

Stephenson NG. 1961. The comparative morphology of the head skeleton, girdles and hindlimbs in the Pygopodidae. *Journal of the Linnean Society of London, Zoology* **44:** 627–644.

Underwood G. 1957. On the lizards of the family Pygopodidae. A contribution to the morphology and phylogeny of the Squamata. *Journal of Morphology* **100:** 207–268.

Wassersug R. 1976. A procedure for differential staining of cartilage and bone in whole formalin fixed vertebrates. *Stain Technology* **51:** 131–134.

Wiens JJ, Slingluff JL. 2001. How lizards turn into snakes: a phylogenetic analysis of body-form evolution in anguid lizards. *Evolution* **55:** 2303–2318.

APPENDIX

Specimens of *B. bicolor* examined: the specimen number is followed by the SVL and the gender (where known).

Neonates: UIS-R-1465, 25.48 mm; UIS-R-1452, 27.52 mm.

Juveniles: UIS-R-1252, 28.18 mm; UIS-R-1451, 30.58 mm; UIS-R-1450, 31.62 mm; UIS-R-1253, 32.50 mm; UIS-R-1456, 36.96 mm (♀); UIS-R-1245, 40.24 mm; UIS-R-1251, 40.32 mm; UIS-R-1462, 42.84 mm; UIS-R-1438, 45.00 mm; UIS-R-1461, 45.72 mm; UIS-R-1455, 47.69 mm; UIS-R-1443, 48.04 mm.

Adults: UIS-R-1458, 49.31 mm (♂); UIS-R-1447, 50.46 mm (♀); UIS-R-1246, 51.28 mm; UIS-R-1247, 52.35 mm; UIS-R-1464, 54.97 mm (♀); UIS-R-1445, 56.73 mm (♀); UIS-R-1460, 57.24 mm (♂), UIS-R-1248, 58.14 mm; UIS-R-1448, 59.00 mm (♂); UIS-R-1437, 61.02 mm; UIS-R-1249, 61.42 mm (♀); UIS-R-1250, 62.05 mm (♂); UIS-R-1439, 62.21 mm; UIS-R-1444, 62.33 mm (♀); UIS-R-1449, 62.40 mm (♂); UIS-R-1441, 63.51 mm; UIS-R-1454, 64.16 mm (♀); UIS-R-1442, 64.30 mm (♂); UIS-R-1440, 64.32 mm; UIS-R-1446, 65.84 mm (♂); UIS-R-1453, 66.27 mm (♂); UIS-R-1459, 67.69 mm (♂); UIS-R-1457, 69.60 (♂); UIS-R-1463, 71.39 mm (♀).